Collision Probability Estimation

Michael R. Phillips,* David K. Geller,† Frank Chavez‡

Utah State University, Logan, Utah, 84321, USA

As small satellites become more common and are assigned increasingly sophisticated missions, their role in proximity operations is also increased. An estimate of the current relative state (position, velocity and often attitude) as well as a prediction of the future relative state is important in close proximity operations. However, it is often insufficient to rely solely on this estimate to predict a collision due to the errors involved in the state estimate. An alternative approach is to determine the probability of a collision. In order to do this, the covariance of the state estimate must also be taken into account. For this reason, it is therefore important to determine a measure of the uncertainty of the position and velocity of both spacecraft. One approach is to conduct a Monte Carlo analysis either onboard or on the ground. Implementing this approach is time consuming and most likely not feasible with current technology. This paper explores the possibility of using covariance propagation onboard a small satellite to perform this uncertainty analysis. Covariance propagation has been shown to be one or two orders of magnitude faster than Monte Carlo analysis. This paper will show how this type of analysis can be used by small satellites for hazard avoidance.

INTRODUCTION

The focus of this paper is a fast technique to estimate the probability of a satellite collision. The technique uses the Clohessy-Wiltshire (CW) equations for state propagation and the discrete Riccati equation for covariance propagation. This technique is valid for use in rendezvous and proximity operations, it can also be used for formation flying and anywhere else that the CW equations are valid.

CLOHESSY-WILTSHIRE EQUATIONS

The CW or Hill's equations are linearized equations that describe the motion of a chaser vehicle relative to a target vehicle. The CW equations assume that the target vehicle is in a near circular orbit. Additionally they assume that the chaser vehicle is in an orbit that is only slightly displaced from that of the target vehicle. The reference frame for the CW equations is centered at the target vehicle with the x-axis pointing up or opposite the gravity vector, the y-axis is in the direction of the local horizontal or roughly aligned with the velocity vector, and the z-axis is normal the orbit plane such that

$$i_z = i_x \times i_y \tag{1}$$

The linearized equations[1] of motion that result from these assumptions are

$$\ddot{x} - 3n^2 x - 2n\dot{y} = 0 \tag{2}$$

$$\ddot{y} + 2n\dot{x} = 0 \tag{3}$$

$$\ddot{z} + n^2 z = 0 \tag{4}$$

where n is the orbital rate of the target vehicle. This can be rewritten in a continuous state space form

$$\dot{\mathbf{x}} = F\mathbf{x} \tag{5}$$

where

$$\mathbf{x} = \begin{bmatrix} r \\ v \end{bmatrix} = \begin{bmatrix} \mathrm{x} \\ \mathrm{y} \\ \mathrm{z} \\ \dot{\mathrm{x}} \\ \dot{\mathrm{y}} \\ \dot{\mathrm{z}} \end{bmatrix} \tag{6}$$

The matrix F is given by

$$F = \begin{bmatrix} 0 & 0 & 0 & 1 & 0 & 0 \\ 0 & 0 & 0 & 0 & 1 & 0 \\ 0 & 0 & 0 & 0 & 0 & 1 \\ 3n^2 & 0 & 0 & 0 & 2n & 0 \\ 0 & 0 & 0 & -2n & 0 & 0 \\ 0 & 0 & -n^2 & 0 & 0 & 0 \end{bmatrix} \tag{7}$$

It can also be written in discrete time form as

$$\mathbf{x}_{i+1} = \Phi_i \mathbf{x}_i \tag{8}$$

where Φ_i is the state transition matrix given in Eq. (9).

*Graduate Student, Mechanical and Aerospace Engineering, 4130 Old Main Hill/UMC 4130

†Assistant Professor, Mechanical and Aerospace Engineering, 4130 Old Main Hill/UMC 4130, Senior Member AIAA

‡Research Engineer, Air Force Research Lab, Albuquerque, NM

$$\Phi_i = \begin{bmatrix} 4-3\cos n\Delta t & 0 & 0 & \frac{1}{n}\sin n\Delta t & \frac{2}{n}(1-\cos n\Delta t) & 0 \\ 6(\sin n\Delta t - n\Delta t) & 1 & 0 & \frac{2}{n}(\cos n\Delta t - 1) & \frac{1}{n}(4\sin n\Delta t - 3n\Delta t) & 0 \\ 0 & 0 & \cos n\Delta t & 0 & 0 & \frac{1}{n}\sin n\Delta t \\ 3n\sin n\Delta t & 0 & 0 & \cos n\Delta t & 2\sin n\Delta t & 0 \\ 6n(\cos n\Delta t - 1) & 0 & 0 & -2\sin n\Delta t & 4\cos n\Delta t - 3 & 0 \\ 0 & 0 & -n\sin n\Delta t & 0 & 0 & \cos n\Delta t \end{bmatrix} \quad (9)$$

COVARIANCE PROPAGATION

The covariance matrix takes the following form

$$P = \begin{bmatrix} P_{rr} & P_{rv} \\ P_{vr} & P_{vv} \end{bmatrix} \quad (10)$$

$$P_{rr} = \begin{bmatrix} \sigma_x^2 & \rho_{xy}\sigma_x\sigma_y & \rho_{xz}\sigma_x\sigma_z \\ \rho_{yx}\sigma_y\sigma_x & \sigma_y^2 & \rho_{yz}\sigma_y\sigma_z \\ \rho_{zx}\sigma_z\sigma_x & \rho_{zy}\sigma_z\sigma_y & \sigma_z^2 \end{bmatrix} \quad (11)$$

$$P_{rv} = \begin{bmatrix} \rho_{x\dot{x}}\sigma_x\sigma_{\dot{x}} & \rho_{x\dot{y}}\sigma_x\sigma_{\dot{y}} & \rho_{x\dot{z}}\sigma_x\sigma_{\dot{z}} \\ \rho_{y\dot{x}}\sigma_y\sigma_{\dot{x}} & \rho_{y\dot{y}}\sigma_y\sigma_{\dot{y}} & \rho_{y\dot{z}}\sigma_y\sigma_{\dot{z}} \\ \rho_{z\dot{x}}\sigma_z\sigma_{\dot{x}} & \rho_{z\dot{y}}\sigma_z\sigma_{\dot{y}} & \rho_{z\dot{z}}\sigma_z\sigma_{\dot{z}} \end{bmatrix} \quad (12)$$

$$P_{vr} = \begin{bmatrix} \rho_{\dot{x}x}\sigma_{\dot{x}}\sigma_x & \rho_{\dot{x}y}\sigma_{\dot{x}}\sigma_y & \rho_{\dot{x}z}\sigma_{\dot{x}}\sigma_z \\ \rho_{\dot{y}x}\sigma_{\dot{y}}\sigma_x & \rho_{\dot{y}y}\sigma_{\dot{y}}\sigma_y & \rho_{\dot{y}z}\sigma_{\dot{y}}\sigma_z \\ \rho_{\dot{z}x}\sigma_{\dot{z}}\sigma_x & \rho_{\dot{z}y}\sigma_{\dot{z}}\sigma_y & \rho_{\dot{z}z}\sigma_{\dot{z}}\sigma_z \end{bmatrix} \quad (13)$$

$$P_{vv} = \begin{bmatrix} \sigma_{\dot{x}}^2 & \rho_{\dot{x}\dot{y}}\sigma_{\dot{x}}\sigma_{\dot{y}} & \rho_{\dot{x}\dot{z}}\sigma_{\dot{x}}\sigma_{\dot{z}} \\ \rho_{\dot{y}\dot{x}}\sigma_{\dot{y}}\sigma_{\dot{x}} & \sigma_{\dot{y}}^2 & \rho_{\dot{y}\dot{z}}\sigma_{\dot{y}}\sigma_{\dot{z}} \\ \rho_{\dot{z}\dot{x}}\sigma_{\dot{z}}\sigma_{\dot{x}} & \rho_{\dot{z}\dot{y}}\sigma_{\dot{z}}\sigma_{\dot{y}} & \sigma_{\dot{z}}^2 \end{bmatrix} \quad (14)$$

The standard deviation of the state elements are represented by σ. The ρ's are the correlation coefficients. As with the state update, the covariance update can also be calculated from a continuous or a discrete equation. These updates are performed with different versions of the Riccati Equation. Eq. $(15)^2$ shows the continuous form of the covariance update with F defined in Eq. (7).

$$\dot{P} = FP + PF^T + Q \quad (15)$$

The process noise, Q, is given by Eq. (16).

$$Q = \begin{bmatrix} 0_{3\times3} & 0_{3\times3} \\ 0_{3\times3} & qI_{3\times3} \end{bmatrix} \quad (16)$$

where q is the process noise strength.

The discrete form of the covariance update is shown in Eq. $(17)^2$ where $\Phi(t)$ is defined in Eq. (9).

$$P_{i+1} = \Phi_i P_i \Phi_i^T + Q\Delta t \quad (17)$$

The process noise, Q, is the same as was given in Eq. (16).

COLLISION METRICS

Two collision probability metrics were explored. The first metric is given by Eq. (18). It basically tells how many standard deviations the centers of each craft are away from each other.

$$M = \frac{\|\mathbf{r}\|}{\sigma_{LOS}} \quad (18)$$

where σ_{LOS} is the extent of the covariance matrix along the line of sight vector between the two spacecraft.

$$\sigma_{LOS} = \frac{1}{\sqrt{i_r^T P_{rr}^{-1} i_r}} \quad (19)$$

This metric does not give an actual estimate of the probability of a collision. Rather it imposes an upper bound on the probabilities of a collision as a function of time. Figure (1) shows the upper limits of collision probability corresponding to values of M.

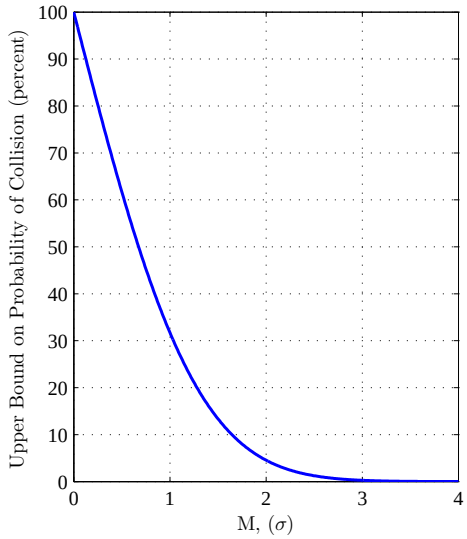

Figure 1. The upper bound for a the probability of a collision for a given standard deviation.

The second metric, p, is a more accurate estimate of the probability of a collision. A spherical keep out region is set around the spacecraft. The point on the sphere with the highest probability density is selected. This is the point, ξ, on the surface of the spherical keep-out region that is in the direction of $\mathbf{r}$. The probability of collision at an instance in time is calculated by multiplying the probability density by the volume of the keep-out region. This probability density, $f(\xi)$, is given by Eq. (20).[3]

$$f(\xi) = K \exp\left\{-\tfrac{1}{2}[\xi - \mathbf{r}]^T P_{rr}^{-1}[\xi - \mathbf{r}]\right\} \qquad K = \frac{1}{(2\pi)^{3/2}|P_{rr}|^{1/2}} \tag{20}$$

where$|P|$ is the determinate of the covariance matrix. The probability, p, of a collision can be calculated using Eq. (21) where $R_{ko}$is the radius of the spherical keep-out region.

$$p = \frac{4}{3}\pi R_{ko}^3 f(\xi) \tag{21}$$

COMPUTATION TIME

The time to calculate the maximum probability of a collision for a few select scenarios can be seen in Table (1).

Table 1. Time in seconds to calculate collision probability metrics.

Orbits	1	4	10
Collision Metric, M	0.0607	0.2417	0.6047
Probability of Collision, p	0.0715	0.2815	0.7054

The computation times displayed are averages over several runs. They were performed on a standard laptop computer running Matlab. The orbits all had a period of 97 minutes, and a step size of 30 seconds was used. These numbers demonstrate the feasibility of calculating the probability of a collision onboard a spacecraft several hours in advance.

Scenarios

Three different scenarios are explored in this report. In all three cases, the initial position errors are $10\,{}^{\mathrm{m}}/_{\mathrm{axis}}$ and the velocity errors are $0.01\,{}^{\mathrm{m/s}}/_{\mathrm{axis}}$.

Football Orbit

The first scenario is a football orbit with a relative path shown in Figs. (2) and (3).

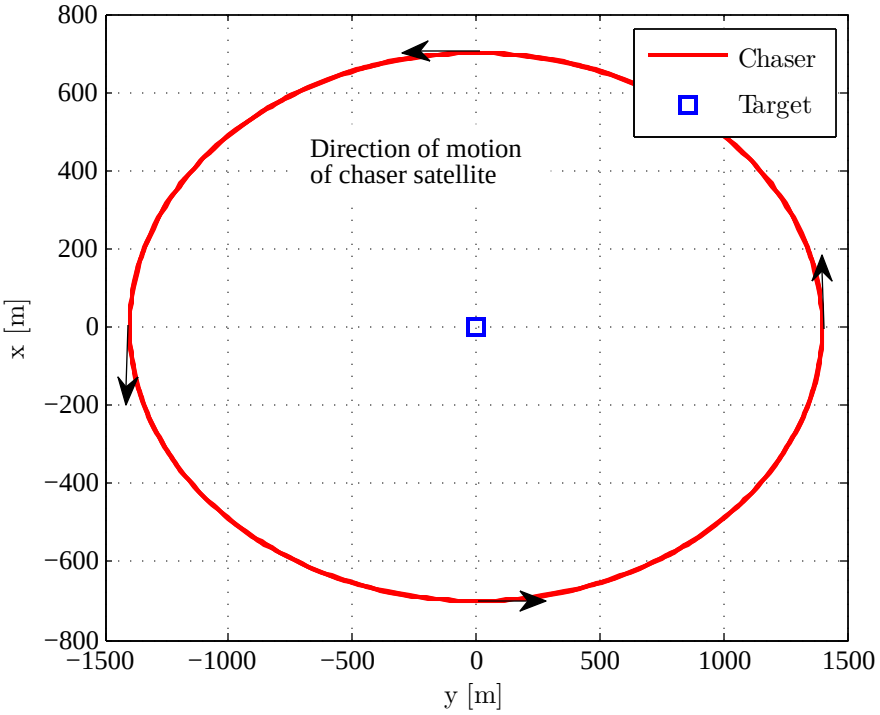

Figure 2. Football orbit propagated for four orbits.

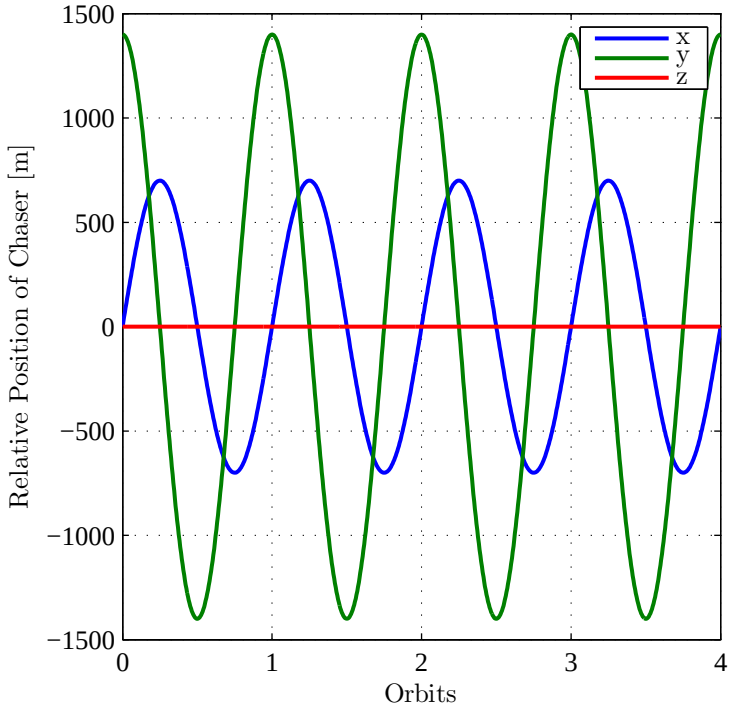

Figure 3. Football orbit propagated for four orbits. Position of chaser is relative to the target satellite.

The variance for the position of the chaser in the x, y, and z directions can be seen in Fig. (4). As can be seen, the component of error in the downrange direction increases roughly linearly with time. This is a result of the growing size of the error ellipse in the downrange direction that can be seen in Fig. (5). The oscillatory components in both the downrange and radial directions are due to orbital mechanics.

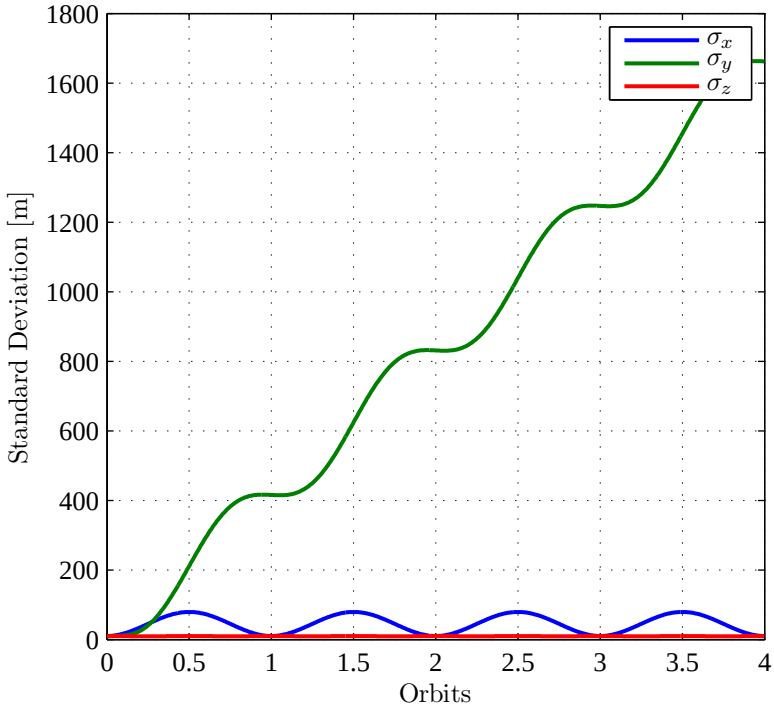

Figure 4. Standard deviations of position propagated for four orbits.

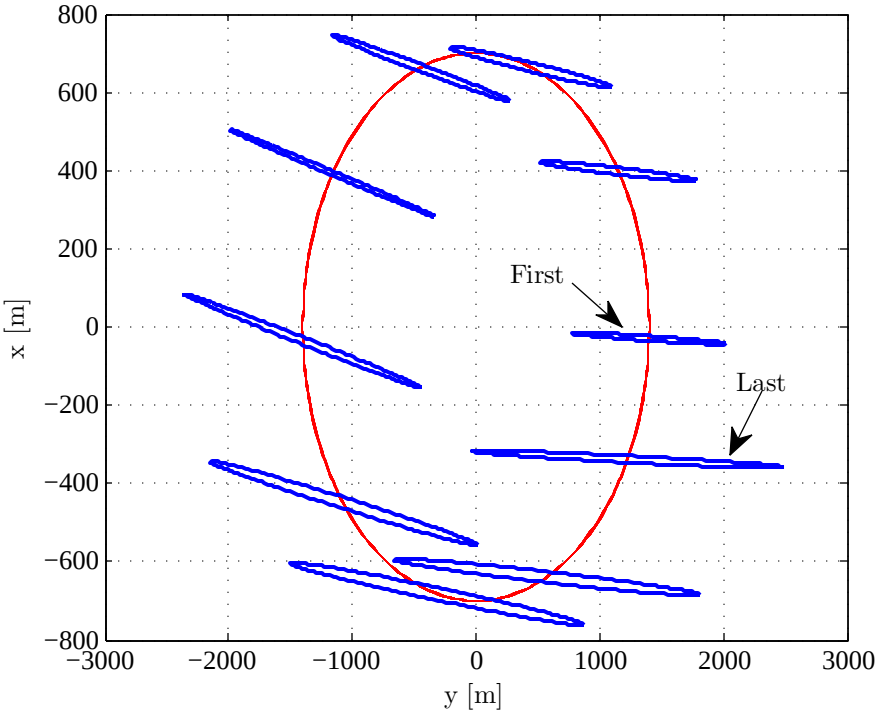

Figure 5. Error ellipsoid and chaser path propagated for a single orbit.

Figure (6) shows the collision metric, M, for this orbit. Higher numbers indicate a lower probability of collision. Comparing to figure Fig. (1), the probability of a collision over the four orbits is quite low and reached a maximum probability of $p \leq 0.172$ for $m = 1.37$ at 2.5 orbits. The metric p is shown in Fig. (7). The predicted probability for a collision is again low, and agrees with the results obtained using the collision metric M.

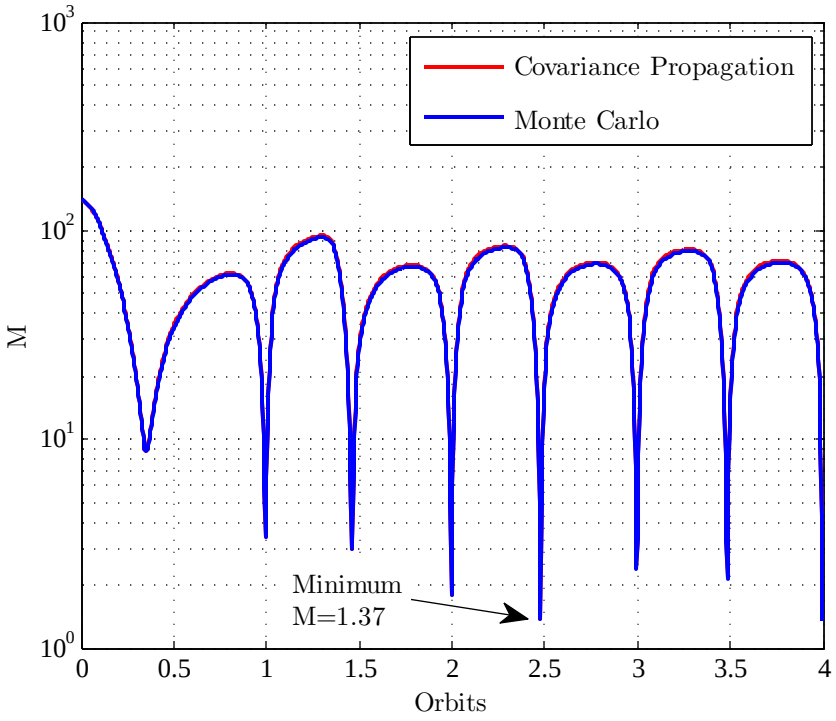

Figure 6. Collision metric propagated for four orbits.

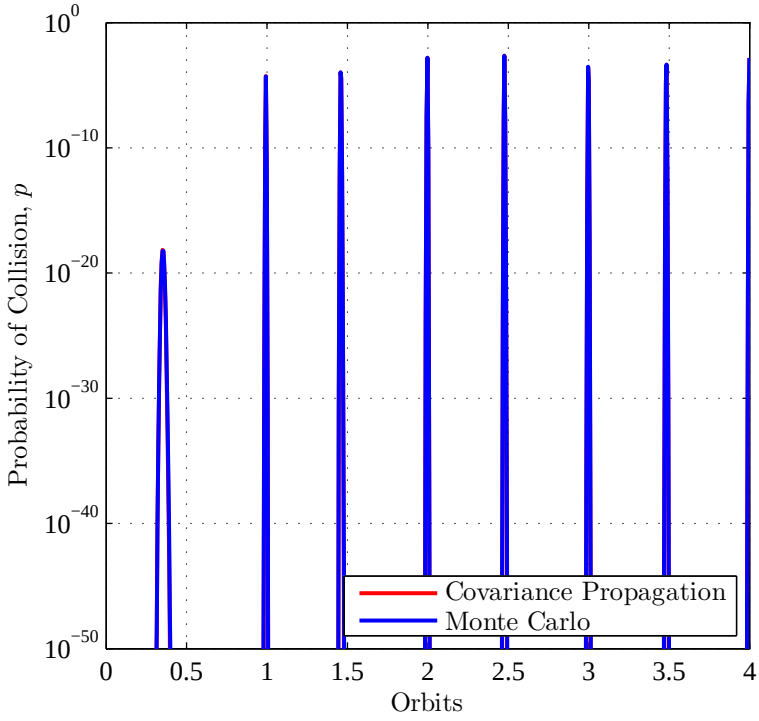

Figure 7. Probability of collision propagated for four orbits.

Overhead Flyby

The second scenario is an overhead flyby with a relative path shown in Figs. (8) and (9).

It is interesting to note that the covariance doesn't change from the previous case due to the time-invariant nature of the dynamics. The variance for the position of the chaser in the x, y, and z directions can therefore be taken from Fig. (4). As can be seen the component of error in the downrange direction increased roughly linearly with time. This is a result of the growing size of the error ellipse in the downrange direction that can be seen in Fig. (10).

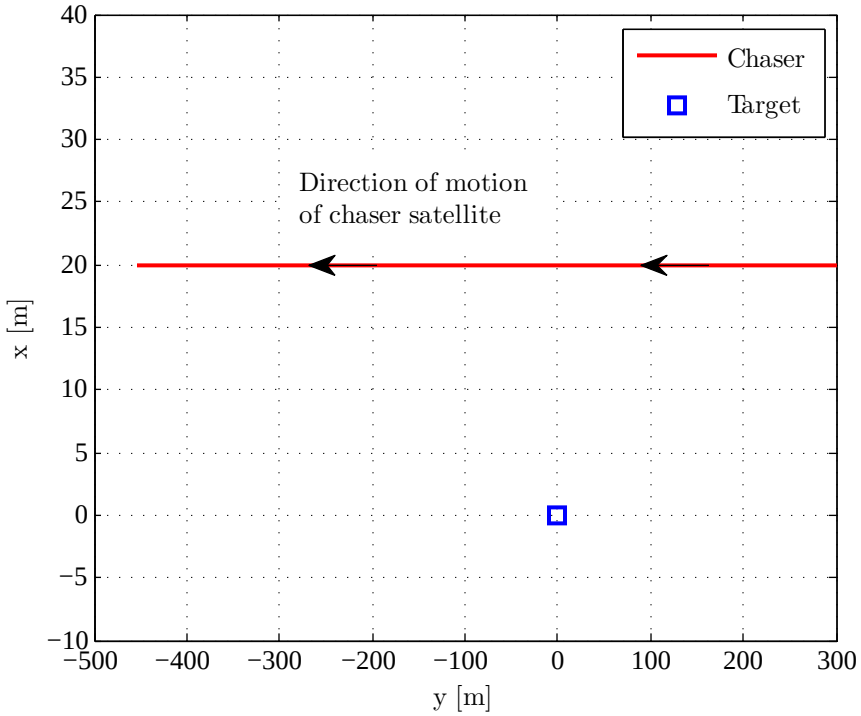

Figure 8. Overhead flyby orbit propagated for four orbital periods.

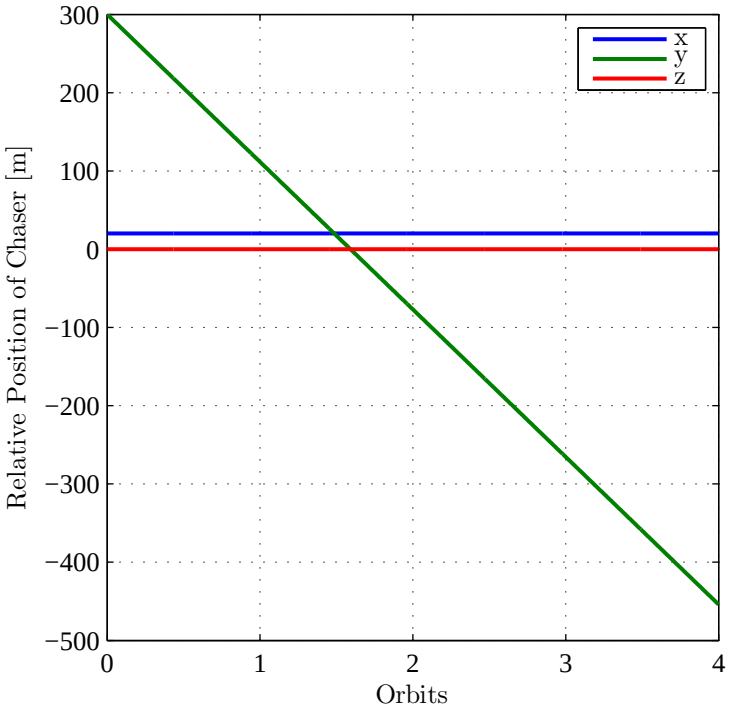

Figure 9. Overhead flyby orbit propagated for four orbital periods.

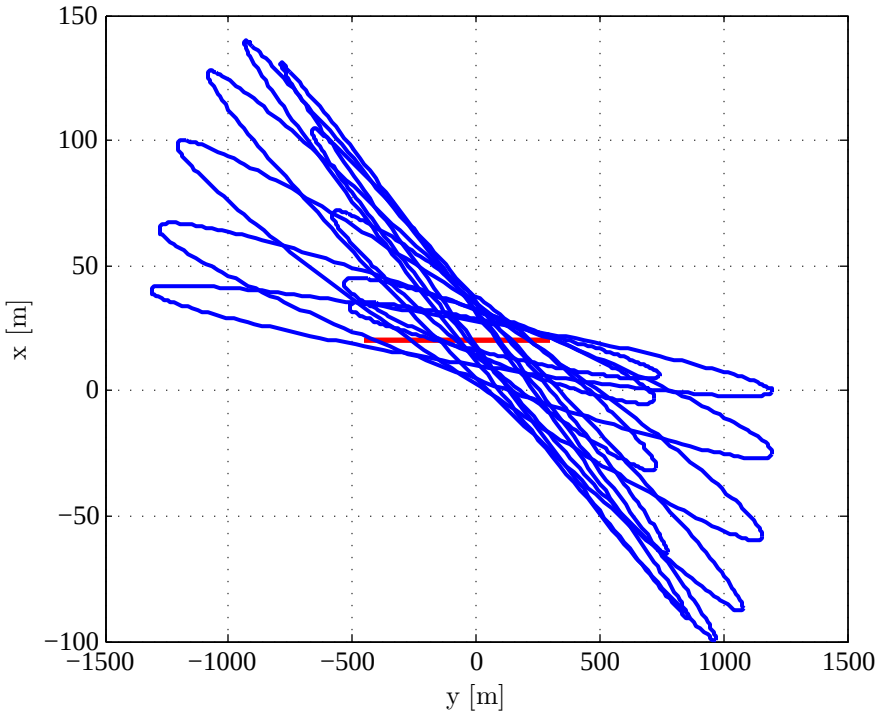

Figure 10. Error ellipsoid and chaser path propagated for a single orbit.

Figure (11) shows the collision metric for this same orbit. Higher numbers indicate a lower probability of collision. As can be seen by Fig. (11) and comparing to figure Fig. (1) the probability for the orbit is quite high. The maximum probability occurs at $t = 3.5$ orbits and has a probability $p \leq 0.791$ for $M = 0.265$. It should be noted that the maximum probability of a collision does not occur at the point of closest approach, as one would think, but actually occurs later. This can is easily explained by the fact the the error ellipse is growing faster than the satellites are distancing themselves from one another. The conservative estimate for the probability of collision is shown in Fig. (12). The predicted probability for a collision using this metric is low, $p \leq 0.0135$. This result disagrees with that obtained by using the metric, M. This demonstrates the need for both metrics as a check against each other, and also shows how the metrics lose meaning when the satellites are in very close proximity. The second metric is the one that should be believed in this case. The error ellipse has grown so large that the actual probability of a collision at any point in time remains quite low even though M has a large value.

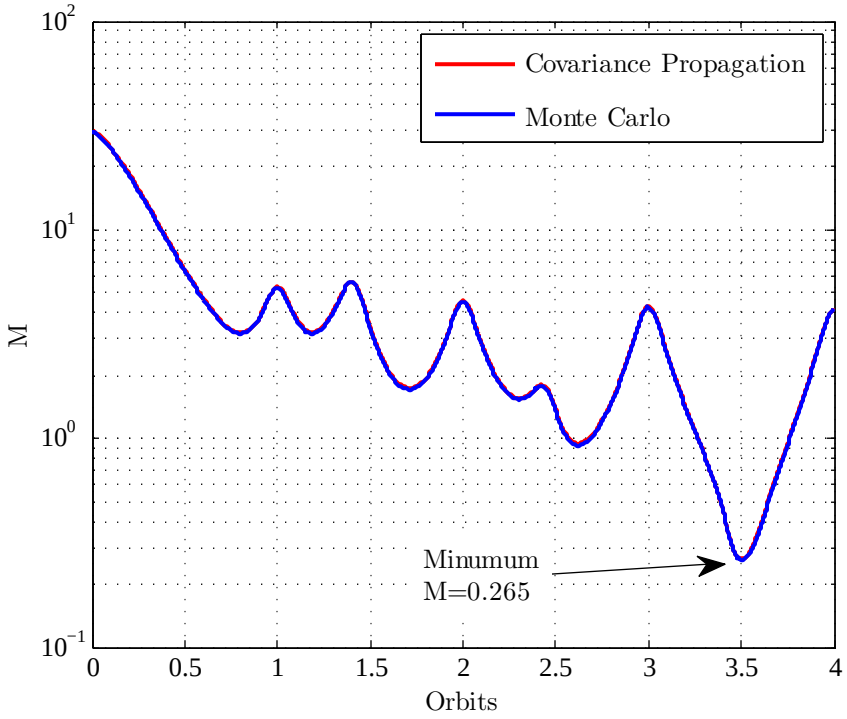

Figure 11. Collision metric propagated for four orbits.

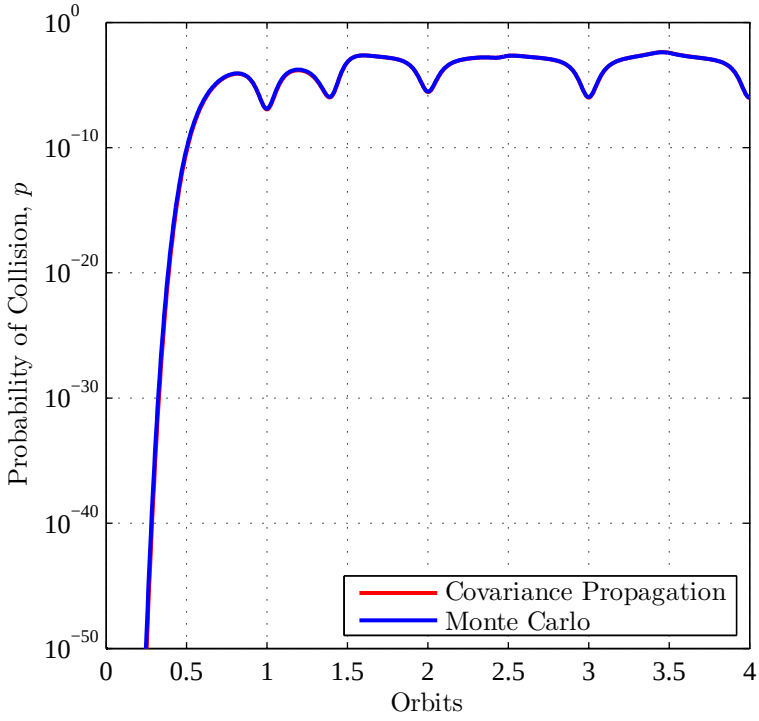

Figure 12. Probability of collision propagated for four orbits.

Football Orbit with High Probability of Collision

The third scenario is another football orbit with a relative path shown in Figs. (13) and (14). This football orbit has a much higher probability of collision than the first because the nominal path passes directly through the target vehicle.

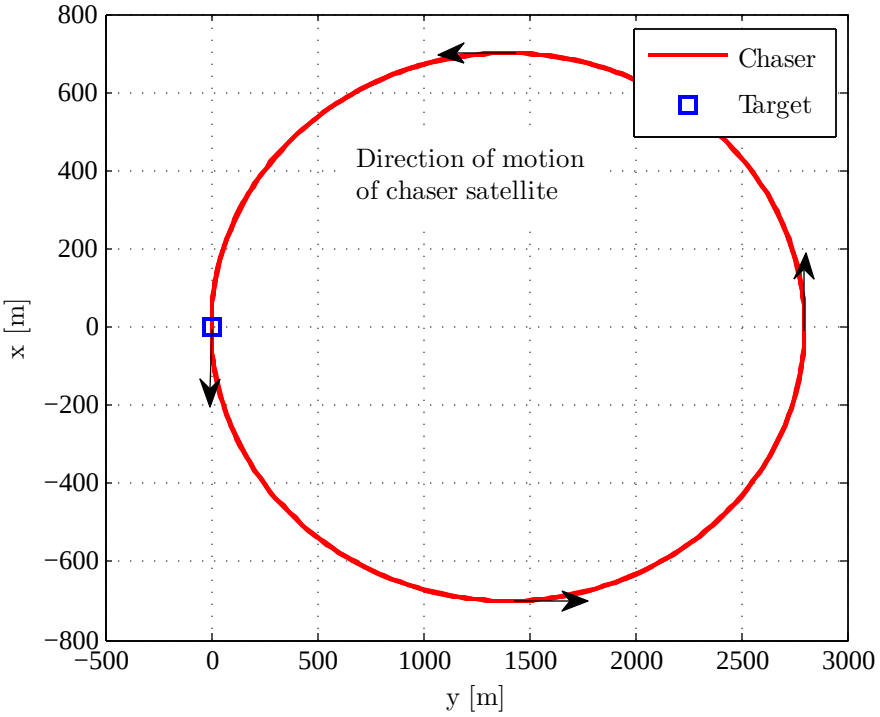

Figure 13. Football orbit propagated for four orbits.

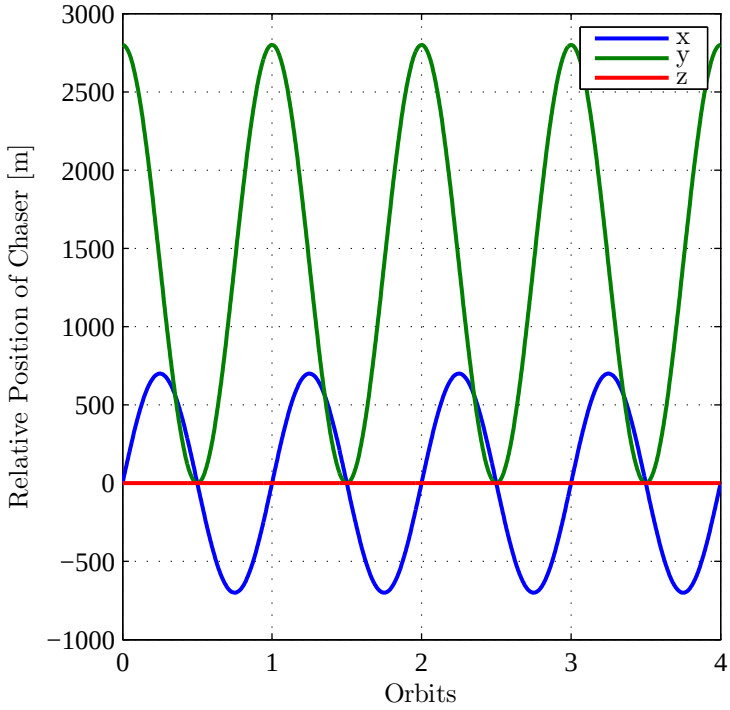

Figure 14. Football orbit propagated for four orbits.

As in the previous case, the covariance does not change. The variance for the position of the chaser in the x, y, and z directions can therefore be seen in Fig. (4).

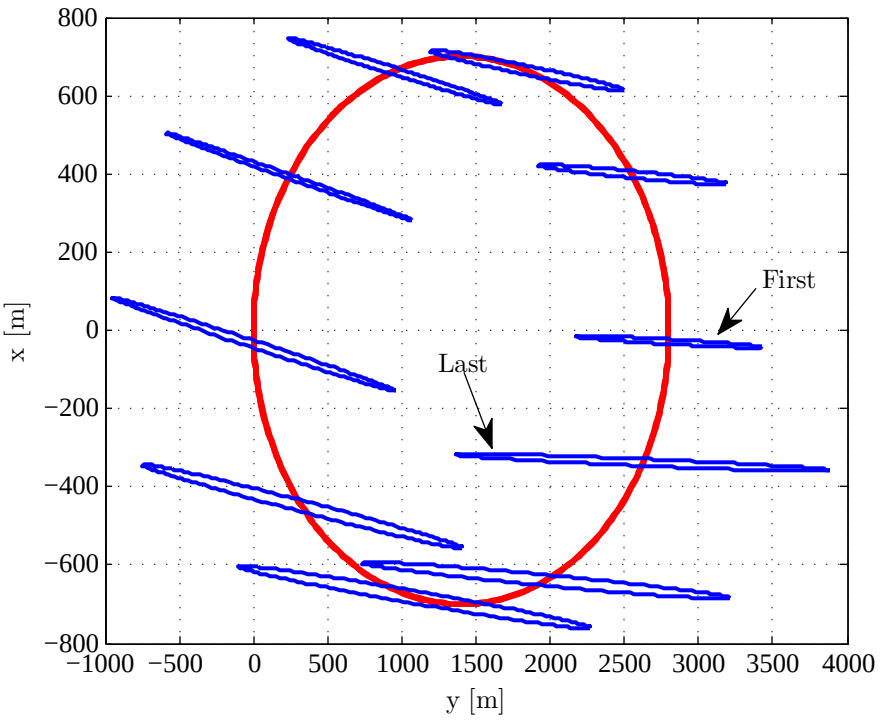

Figure 15. Error ellipsoid and chaser path propagated for a single orbit.

Figure (16) shows the collision metric for this same orbit. As can be seen by Fig. (16). and comparing to figure Fig. (1). the probability for the orbit is quite a bit higher than it was for the previous case. The maximum probability occurs at $t = 3.5$ orbits and has a probability $p \leq 0.977$ for $M = 0.029$. The conservative estimate for the probability of collision is shown in Fig. (17). The predicted probability for a collision is also slightly higher than in the previous cases. The same explanation given in the previous scenario for the conflicting results produced by the metrics is also valid here.

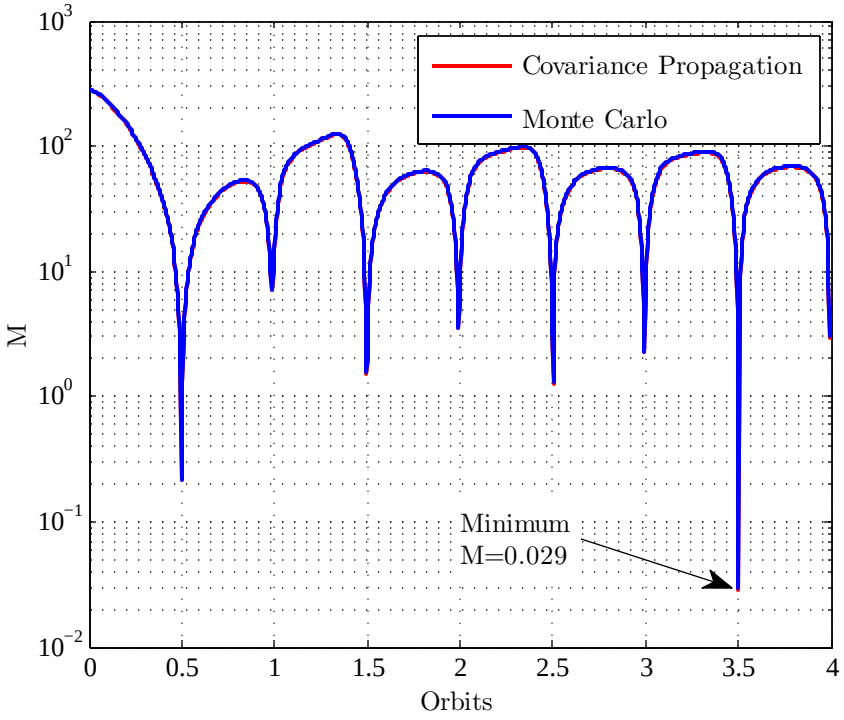

Figure 16. Collision metric propagated for four orbits.

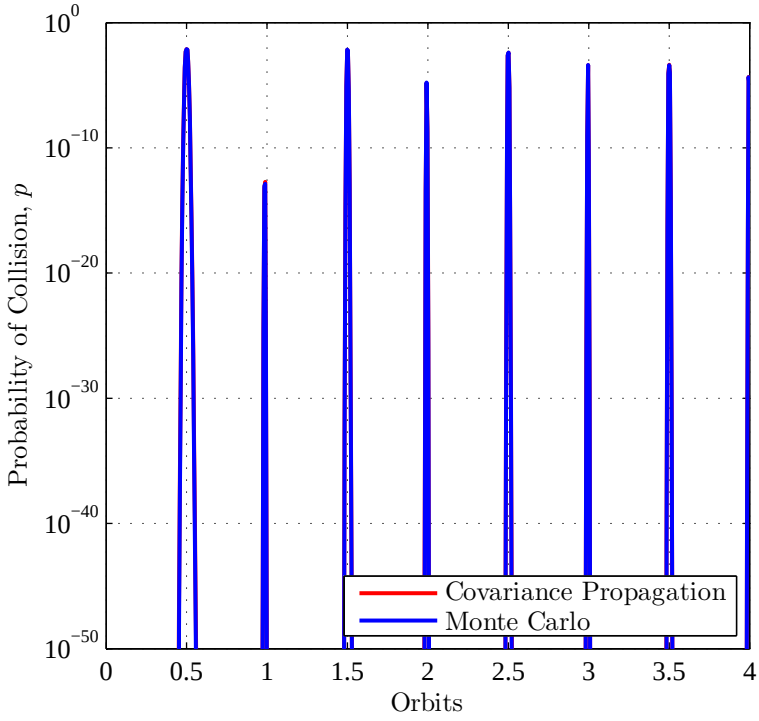

Figure 17. Probability of collision propagated for four orbits.

VALIDATION WITH MONTE CARLO

A Monte Carlo simulation was ran in parallel for all three scenarios to verify the results obtained from the covariance propagation. As can be seen in Figs. (6), (7) , (11), (12), (16) and (17) the results obtained by the two methods agree very closely with each other. It is therefore reasonable to assume that the covariance propagation is producing accurate results.

CONCLUSION

The two metrics discussed in this paper give beneficial insight into the probability that a collision will occur. They also provide a good check against each other for validation purposes and to further help avoid a collision. Each one has its advantages, disadvantages and limitations. Both are conservative estimates of collision probability. This assumes that the nominal estimate of position is outside the keep out zone. Neither method attempts to obtain an aggregate probability over time to get a total estimate for collision probability. Both metrics rely on the CW Equations which have limitations as was previously discussed. However there are many situations where these equations are valid, and it is in these situations when we are most concerned with the chance that of a collision. This method is very quick which increases its utility, and as long as the probability of a collision stays low they do give a good upper bound to the probability.

References

[1]Curtis, H. D., *Orbital Mechanics for Engineering Students*, Elsevier Aerospace Engineering Series, Elsevier Butterworth-Heinemann, 1st ed., 2005.

[2]Crassidis, J. L. and Junkins, J. L., *Optimal Estimation of Dynamic Systems*, Chapman & Hall/CRC Applied Mathmatics and Nonlinear Science Series, Chapman & Hall/CRC, 2004.

[3]Maybeck, P. S., *Stochastic Models, Estimation, and Control*, Vol. 141-1 of *Mathmatics in Science and Engineering*, Navtech Book & Software Store, 1994.